Rheology of (Carboxymethyl)cellulose with Xanthan Gum Properties

J. G. Westra

AKZO Corporate Research Laboratories, Velperweg 76, 6800 AB Arnhem, Netherlands.
Received December 4, 1987; Revised Manuscript Received April 29, 1988

ABSTRACT: (Carboxymethyl)cellulose (CMC) with locally a low degree of substitution, in fact a cellulose-*co*-CMC segmented block copolymer, was recently synthesized. The rheological properties of aqueous solutions of these products were quite similar to those of highly pseudoplastic solutions of xanthan gum. The slope B of the Ostwald–De Waele power law equation could be used quite well for characterizing the pseudoplasticity. The temperature dependence of the rheology of these xanthan gum mimicry samples was very similar to that of xanthan and markedly different from that of the usual type of CMC.

1. Introduction

Aqueous solutions of some polysaccharides (e.g., the guar and xanthan gums) show strong pseudoplastic shear-thinning effects. At low shear levels the apparent viscosity may be quite high, even at rather low concentrations, and η drops markedly with increasing shear rate $\dot{\gamma}$. In contrast, similar concentrations of sodium (carboxymethyl)cellulose have nearly Newtonian properties.

Sikkema[1] tried to prepare CMCs with properties similar to xanthan, by grafting dextrin side chains in a random pattern to the cellulosic backbone. Although products with high visosities could be made, this grafting process failed to produce materials with the desired pseudoplasticity.

The rheology and structure of xanthan has been investigated quite thoroughly; cf. recent surveys.[2,3] According to X-ray studies[4-6] the primary structure has a pentasaccharide repeat unit: charged trisaccharide side chains attached to the O-3 atom of alternate glycosyl residues of the cellulosic backbone chain. The internal mannose of the side chain is acetylated and the terminal mannose carries a pyruvate group. The degree of pyruvate substitution depends on the fermentation process and on the strain of the xanthomonas bacteria.

The backbone conformation may result in a more or less ordered secondary structure (helix → coil transformation). The flexibility of the cellulosic chain can be influenced by the temperature and changes in ionic strength. (Xanthan is a polyelectrolyte due to its acetate and pyruvate groups.) Addition of salt to solutions of xanthan in pure water causes a collapse of the side chains toward the backbone (screening of charges), thus creating a rodlike conformation, with intermolecular association by hydrogen bonding. At higher concentrations indeed a cholesteric liquid crystal phase has been observed,[7] with permanent or stress-induced birefringe (depending on the concentration level).[8] About the tertiary structure there has been much debate. From X-ray work on oriented xanthan, Moorehouse[6] suggested a single helical structure. A later interpretation[9] of the same data yielded a double-stranded helix. Also, the electron micrograph work of Holzwarth and Prestridge[10] showed double (as well as partly unraveled right-hand twisted) helices. This EM work—on native, denaturated, and renaturated material—was firmly supported by sizing experiments with millipore filters. More recent EM work[11] showed both single- and double-stranded chains, as well as partly unraveled helices. The tertiary structure of xanthan seems to depend on the manufacture process of the pertinent sample, on the solution procedure, and on salinity level and temperature. At least in many cases xanthan exists in solution as a double-chain tertiary structure of extremely stiff macromolecules, with strong intermolecular associations. The peculiar rheological properties of aqueous solutions of xanthan seem to be due to a superstructure of large rigid rods. There exists some similarity of this microstructure with a staple yarn, built up from much shorter fiber elements. This inspired Sikkema and Janssen[12] to attempt another approach to xanthan imitation. An association should align the cellulosic backbones into bundles with an effective length largely exceeding the dimensions of the CMC molecule. This concept was realized by adjusting the alkalinity to a lower level just before the carboxymethylation step, so causing a partial recrystallization of the alkali cellulose. The microcrystals thus created protect the cellulose from substitution. In this way a "block copolymer" is obtained, with regions of poorly substituted cellulose. Multistranded CMC colloidal fibers are thus produced in the solutions by physical cross-linking, acting via the nonsubstituted cellulose blocks. This approach, which turned out to be successful, leads to a CMC with a pseudoplasticity comparable with that of xanthan (though not yet fully reaching that level). Evidently, the characterization of the pseudoplasticity of the XGM samples (XGM = xanthan gum mimicry) is an important tool in the selection of proper process conditions. The effect of temperature on the rheology of xanthan solutions is small. For certain applications of XGMs a similar temperature dependence might be desirable, so this feature was also investigated.

2. Evaluation of Pseudoplasticity

In rheological plots (generally presented on logarithmic scales) shear-thinning objects show a decrease of apparent viscosity η with increasing shear rate $\dot{\gamma}$. Figure 1a presents the decrease of η from a Newtonian level η_0 toward a secondary level η_∞. Evidently these sigmoid curves have a point of inflection, which is also the case in shear-stress versus shear-rate plots (Figure 1b). In the region around this inflection point a linear correlation of log η and log $\dot{\gamma}$ (or log τ and log $\dot{\gamma}$) exists. Then the system obeys the Ostwald–De Waele equation $\log \eta = A + B \log (\dot{\gamma})$, or "power law" $\tau = a(\dot{\gamma})^k$, where evidently $B + k = 1$. This power law linearity in the log–log plots is restricted just to a certain range of shear rates. The pertinent range obviously depends also on the severity of straight line requirements. Figure 8 in the publication of Whitcomb and Macosko[13] shows plots for 1000, 2000, 3500, and 10 000 ppm aqueous xanthan. Only the 10 000 ppm case is a straight line, and evidently even for one subject the power law region is a function of concentration (this region being just a reasonably straight part of an intrinsically curved relation).

We observed for 1% xanthan solutions an excellent linearity over 5 decades of shear rate, from $\dot{\gamma} = 0.01$ up to 1000 s^{-1}. Evaluation of pseudoplasticity with the power law is no problem for xanthan. Another aspect is the viscosity level at a well-defined shearing level. For any one type of sample the parameters A and B are rather well correlated, so in an investigation concerned with pushing

0024-9297/89/2222-0367$01.50/0

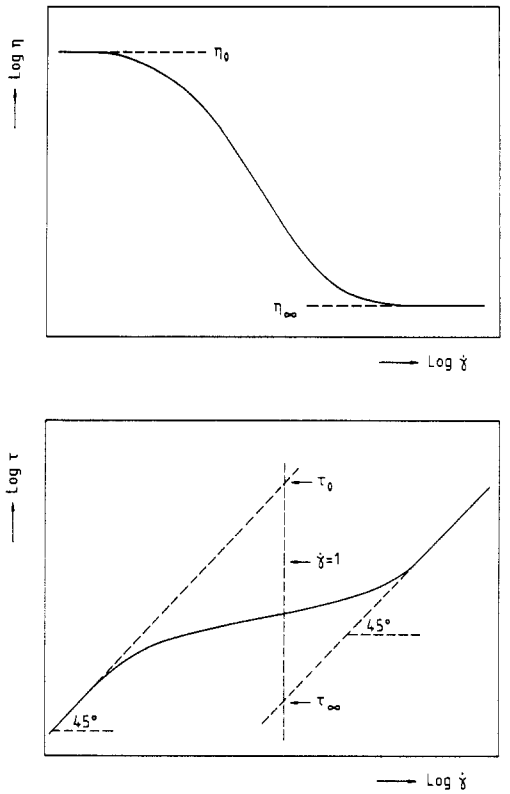

Figure 1. (a, Top) Plot of log viscosity versus log shear rate for a pseudoplastic (shear thinning) substance. (b, Bottom) Plot of log shear stress versus log shear rate.

up the pseudoplasticity level it is sufficient to observe just the slope parameter B (or power law exponent k). The XGM samples always showed a less perfect linearity than xanthan over the same shear rate interval. However, for XGMs the curvature always remained quite small (cf. sections 4 and 5).

According to our experience, curves with a slight curvature can be fitted quite well by an exponential relation. For the log τ – log $\dot{\gamma}$ plots this results in $\log \tau = a - b(\dot{\gamma})^c$, with three positive parameters. The slope of a tangent line at any point (defined by its shear rate $\dot{\gamma}$) is then $S = 2.303bc(\dot{\gamma})^{-c}$, and the curvature is given by $cS(1 + S^2)^{1.5}$. For several XGM samples the rheological curves were measured from $\dot{\gamma} = 0.1$ up to 1000 s^{-1}.

The Ostwald slope and the tangential slope and curvature at $\dot{\gamma} = 10$ s^{-1} (the midpoint in the log presentation) were evaluated. Figure 2 shows the excellent correlation of these data. Evidently the tangential slope at the midpoint of these curves may be substituted quite well by a power law slope, which assumes the rheological curve to be a straight line. And of course the evaluation of a power law slope is quite simple in computation, e.g., by measuring data at 1 and 100 s^{-1} or at 0.1 and 1000 s^{-1}. So this became our standard procedure for establishing the pseudoplasticity of XGM samples.

3. Experimental Section

A modified Sangamo Weissenberg rheogoniometer with a cone–plate measuring system was used for most measurements. This instrument was coupled to a Hewlett-Packard HP86 personal computer. Rheograms at low shear levels (up to 2 s^{-1} with a 1° cone) were always recorded with the moving coil motor, having a very fast and accurate response to a programmed voltage sweep. To obtain also proper noise levels at higher shear levels (operating with the original motor and gear box) plates 10 cm in diameter were used to obtain relatively large signals. Moreover, a further noise reduction was achieved by averaging over 16 individual readings. One rheogram (100 data points up and 100 down) was

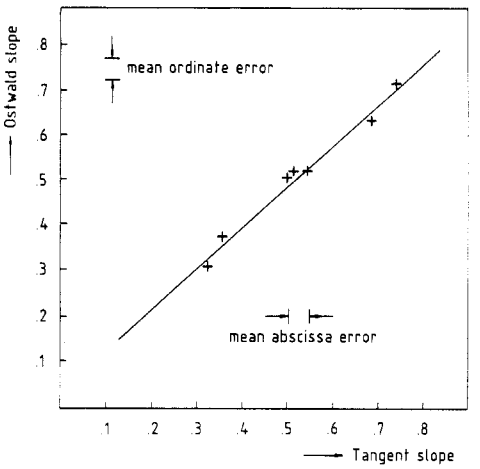

Figure 2. Ostwald slope versus tangential slope at $\dot{\gamma} = 10$ s^{-1} for several XGM samples.

recorded in 3 min. Centrifugal effects (at the 10-cm plates) sometimes caused a small loss of sample at 1300 s^{-1} shear rate, so a safe maximum for the Weissenberg is 1100 s^{-1}. For work at elevated temperatures (up to 100 °C) the Carri-Med CS100 constant-shear-stress rheometer, coupled to an Apple IIC computer, was more suitable. This instrument has a thermostated bottom plate (hot water circulation) and a Peltier element. Either complete rheograms at a well-defined temperature can be recorded (τ sweep and $\dot{\gamma}$ measurement) or the shear rate is measured (at constant τ), yielding a viscosity output in a temperature sweep.

In the Carri-Med the maximum plate diameter is 6 cm. So centrifugal effects are smaller. The maximum rotation speed is 50 rad/s. With 1% solutions of xanthan or XGMs, the shear rate maximum comes close to 5000 s^{-1}. In terms of signal-to-noise, the Weissenberg (with its moving coil motor) is superior to the Carri-Med in the lower ranges. At higher rates both instruments can always be operated at satisfactory noise levels.

For each sample (generally 1 wt % solutions) one rheogram was recorded up to 2 s^{-1} and a second one up to 180 s^{-1}. The shear-stress values at 1 and 100 s^{-1} were used to calculate η_1 and slope parameter B in the Ostwald equation $\log \eta = \log \eta_1 - B \log \dot{\gamma}$. (Cf. the end of section 2). Sometimes also a complete τ–$\dot{\gamma}$ picture (0.1–1000 s^{-1}) was obtained in addition to the characterization by B data.

4. Rheological Results Obtained with XGM Samples

The preparation of XGM always starts with a complete destruction of crystallinity (high alkalinity). To create local protection against the final etherification step, a partial recrystallization is then evoked by decreasing the alkalinity.[12] The reactions were carried out either in a slurry (in 85% isopropyl alcohol) or in a kneader ("dry phase"). In the slurry process the etherification was usually carried out by adding only chloroacetic acid (=MCA) or sometimes by using a mixture of MCA and acrylamide. The reproducibility of the slurry process was better and the clarity of the aqueous solutions nearly perfect. The dry-phase products are just acceptable. Also the shear-thinning performance of slurry products is in general slightly better. Figure 3 shows the rheology of several XGM samples (codes refer to the tables in the preceding paper[12]), together with xanthan and pure water. The latter gives a Newtonian straight line. The 1% aqueous solution of xanthan shows a power law behavior and also gives a straight line. The XGM lines are always slightly curved.

XGM IV-1 is a dry-phase product of rather poor performance ($B = 0.24$).

5. Discussion of XGM Pseudoplasticity

Slurry reactions with Buckeye ER 4500 linters yielded products with B up to 0.47 (XGM I-5), being certainly an

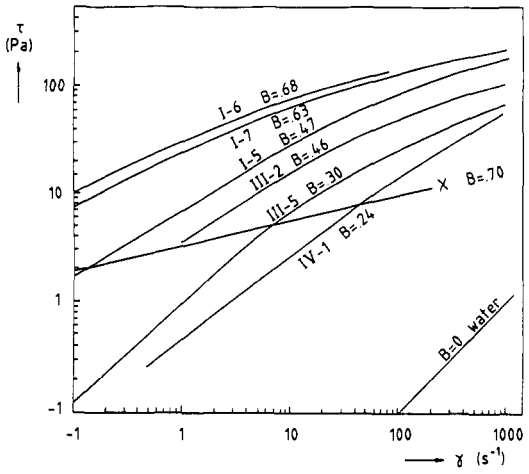

Figure 3. log shear stress versus log shear rate for xanthan solution and various XGM samples.

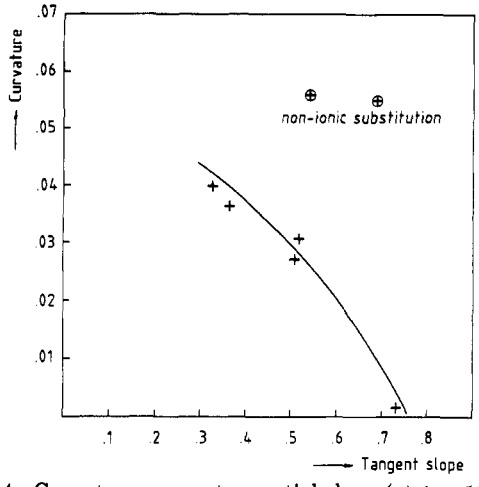

Figure 4. Curvature versus tangential slope (at $\dot{\gamma} = 10\ s^{-1}$) in log τ–log $\dot{\gamma}$ plots of XGM samples.

impressive achievement compared with the dextrin-grafted products. (The previously reported products[1] generally had $B = 0.10$ and only some reached the 0.15 level. All were situated in Figure 3 in the area between IV-1 and pure water.) With the same slurry process, but with ER 8500 linters, products with $B = 0.63$ and $B = 0.68$ were obtained. The B values of these XGMs already approach the value of xanthan (compare with $B = 0.80$ reported for 1.5 and 2% solutions[14] and with $B = 0.70$ measured by us at a 1% solution).

The rheological behavior of xanthan is not the only standard for XGM synthesis. Also the salt resistance can be important for some applications (oil drilling liquids). Nonionic substitution (with acrylamide) had a positive effect on salt resistance, but at the expense of some pseudoplasticity. Compare III2 with I6 and I7 with the same type of cellulose (B values are in Figure 3). Moreover, hydrolysis of the amide functionality caused a further decrease in pseudoplastic behavior (III2 was transformed into III5, the latter with a lower B level). Figure 4 gives a plot of curvature versus tangential slope. For normal XGMs there is a fair correlation (the two divergent data points being related to the different manufacturing process with acrylamide).

6. Evaluation of the Temperature Dependence of Viscosity

In section 2 it was already mentioned that xanthan has an order–disorder transition (helix–coil), which is also sensitive to the electrolyte content of the solutions. In the absence of salt the viscosity decreases slightly between 20 and about 40 °C. Then η rises sharply, and beyond about 75 °C the η decline is resumed. Cf. also Figure 6 in an early publication.[15]

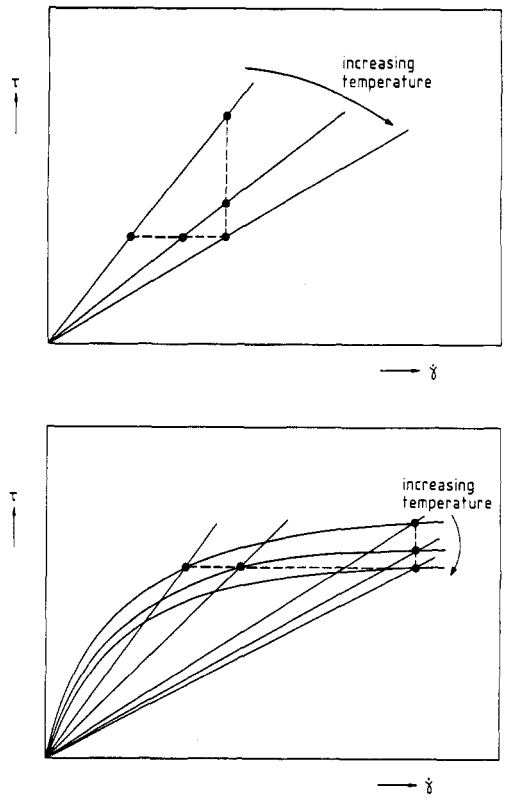

Figure 5. (a, Top) Shear stress versus shear rate at different temperatures for a Newtonian system. (b, Bottom) Shear stress versus shear rate for a pseudoplastic system.

For a Newtonian material it makes no difference if η has been measured as $\tau = f(T)$ at constant $\dot{\gamma}$ or as $\dot{\gamma}$ data at constant τ (cf. Figure 5a). But for a pseudoplastic substance the change of *apparent* viscosity with temperature is evidently much larger for measurements at constant τ than for data measured at constant $\dot{\gamma}$ (cf. Figure 5b). Evaluation of the temperature dependence of η (usually expressed as an activation energy of flow, derived from the slope of an Arrhenius plot) will give two types (E_τ and $E_{\dot{\gamma}}$) in the case of a pseudoplastic substance. See earlier publications.[16,17] From the definitions $\ln (\tau/\dot{\gamma})_{\dot{\gamma}} = A + (E_{\dot{\gamma}}/RT)$ and $\ln (\tau/\dot{\gamma})_{\tau} = A + (E_\tau/RT)$ it is obvious that the ratio of E_τ and $E_{\dot{\gamma}}$ is given by the absolute value of $(d \ln \tau)/(d \ln \dot{\gamma})$. For a Newtonian substance E_τ and $E_{\dot{\gamma}}$ are evidently identical. And if for a pseudoplastic system the Ostwald–De Waele equation holds, then $E_{\dot{\gamma}} = kE_\tau$, where k is the power law index.

Narayan and Ramasubramanium[14] studied the effect of temperature (20–40 °C, in the lower range) on the rheology of aqueous xanthan solutions, but also for several other polysaccharides (guar, alginate, and karaya gums and sodium CMC). All systems obeyed the power law quite reasonably ($r = 0.97$–0.99 for the log τ–log $\dot{\gamma}$ plots). Data for the various temperatures were reported as A and B values of the $\log \eta = A - B \log \dot{\gamma}$ relation, as well as activation energies of flow (in kilocalories per mole). As the basic data had been measured with a Haake Rotovisko at various shear rates ($\dot{\gamma} = 7$–$1140\ s^{-1}$), obviously the E values are $E_{\dot{\gamma}}$ data. (Evidently the authors were not aware of the existence of two types of E parameters in pseudoplastic objects.)

The $E_{\dot{\gamma}}$ data of xanthan and guar gums were quite low (about 4 kJ/mol), in sharp contrast to the level 20–30

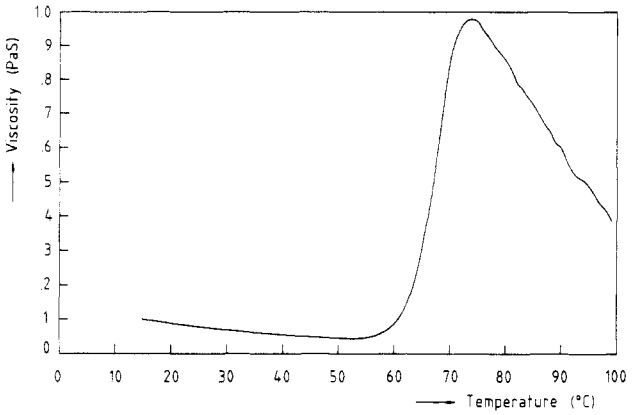

Figure 6. Viscosity dependence on temperature for xanthan (τ = constant).

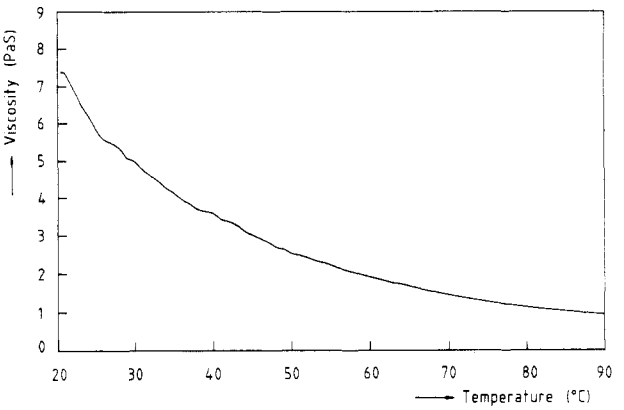

Figure 7. Viscosity dependence on temperature for XGM sample 17 (τ = constant).

kJ/mol for the other polysaccharides. Thus the Indian authors concluded highly significant differences in interaction mechanisms. However, the E_τ data, which we estimated form $E_\dot{\gamma}$ and the reported B data, yield less conclusive results. For guar gum the $E_\dot{\gamma}$ value had to be multiplied by 10, for xanthan by 5, and for CMC by 2.5, whereas the $E_\dot{\gamma}$ data of alginate and karaya gums had to be only doubled. Thus the separation of guar and xanthan from the other items is far less significant in E_τ!

As reference for our measurements on XGMs the Indian publication gives $E_\dot{\gamma}$ = 3.0 ± 1.5 kJ/mol and E_τ = 20.7 ± 1.0 kJ/mol for xanthan below the transition point and for CMC 25–30 and 50–60 kJ/mol, respectively.

7. Results from Variable-Temperature Measurements on XGMs

Prior to the measurements on XGMs, xanthan was also studied. With the Carri-Med the η–t trace of a 1.7% xanthan solution was recorded (15–99 °C, τ = 45 Pa); see Figure 6. The viscosity decreases with increasing temperature, with a sharp rise in the 60–70 °C interval, due to the helix–coil transformation. From the 75–95 °C region of Figure 6 a value of 37 kJ/mol was derived for E_τ. And from a similar recording at τ = 25 Pa (for getting higher and more accurate η data) for the 20–50 °C region an E_τ value of 21.6 ± 0.7 kJ/mol was calculated.

Figure 7 shows the trace for sample I-7 (the top XGM of the slurry process), recorded at τ = 80 Pa. A similar trace was obtained for a dry-phase XGM (B = 0.38, not high quality). The viscosities were about 1 decade lower; the trace was recorded at τ = 25 Pa. In accordance with the different nature of XGM and xanthan there is no η jump. Values of E_τ of 27 (I-7, up to 75 °C) and 34 kJ/mol (the dry-phase sample, up to 50 °C) were calculated from the pertinent traces of these XGMs.

8. Discussion

For xanthan the experimental E_τ value below the transition point (21.6 ± 0.7 kJ/mol) is in good agreement with 20.7 ± 1.9 calculated by us from the literature.[14]

The E_τ value above the transition point (37 kJ/mol) cannot be compared with literature data. However, it is of the same magnitude as E_τ below the transition point. And this is quite conceivable: if the transition is taken as the dissociation of a double-helix structure,[10] then the viscosity response to temperature will not be very different for both systems.

The E_τ level of XGMs (27 kJ/mol for a top XGM and 34 kJ/mol for an intermediate type) is closer to E_τ of xanthan (22 in the lower range and 37 kJ/mol for the upper temperatures) then to E_τ of normal-type CMC (50–60 kJ/mol, as estimated in section 6 of ref 14).

Evidently the block-copolymer-type CMC, proposed by Sikkema[12] to mimic the rheology of xanthan, is also rather close to xanthan in terms of temperature dependence. The similar rather low level of E_τ indicates *a strong intermolecular association*—as in xanthan. Thus the concept of physical network creation, acting between glycosyl residues of a low degree of substitution, yields quite promising results.

Complete matching of properties is impossible with a material of a different molecular structure. A reasonable matching is only possible within limited regions, and some properties will be imitated less well.

Registry No. CMC, 9004-32-4; xanthan gum, 11138-66-2.

References and Notes

(1) Sikkema, D. J. *J. Appl. Polym. Sci.* **1985**, *30*, 3523.
(2) Rochefort, W. E.; Middleman, S. *J. Rheol. (N.Y.)* **1987**, *31*, 337.
(3) Richardson, R. K.; Ross-Murphey S. B. *Int. J. Biol. Macromol.* **1987**, *9*, 257.
(4) Jansson, P. E.; Kenne, L.; Lindberg, B. *Carbohydr. Res.* **1975**, *45*, 275.
(5) Melton, L. D.; Mindt, L.; Rees, D. A.; Sanderson, G. B. *Carbohydr. Res.* **1976**, *46*, 245.
(6) Moorehouse, R.; Walkinshaw, M. D.; Arnott, S. *ACS Symp. Ser.* **1977**, *No. 45*, 90.
(7) Milas, M.; Rinaudo, M. *Polym. Bull. (Berlin)* **1983**, *10*, 271.
(8) Lim, T.; Uhl, J. T.; Prudhomme, R. K. *J. Rheol. (N.Y.)* **1984**, *28*, 367.
(9) Okuyama, K.; Arnott, S.; Moorehouse, R.; Walkingshaw, R. D.; Edkins, E. D. T.; Wolf-Ullish, C. *ACS Symp. Ser.* **1980**, *No. 141*, 411.
(10) Holzwarth, G.; Prestridge, E. B. *Science (Washington, D.C.)* **1977**, *197*, 757.
(11) Stocke, B. J.; Elgsaeter, A.; Smidsrod, O. *Int. J. Biol. Macromol.* **1986**, *8*, 217.
(12) Sikkema, D. J.; Janssen, H. *Macromolecules*, preceding paper in this issue.
(13) Whitcomb, P. J.; Macosko, C. W. *J. Rheol. (N.Y.)* **1978**, *22*, 493.
(14) Narayan, K. S.; Ramasubramanium, V. *Indian J. Technol.* **1982**, *20*, 333.
(15) Jeanes, A.; Pittsley, J. E.; Senti, F. R. *J. Appl. Polym. Sci.* **1961**, *5*, 519.
(16) Semjonow, V. *Adv. Polym. Sci.* **1968**, *8*, 387.
(17) Bestul, A. B.; Belcher, H. V. *J. Appl. Phys.* **1953**, *24*, 696.